Analysis of magmatic productivity at the Rochambeau Rifts, northern Lau back-arc Basin

M. Ryan[1], M.D. Hannington[1], A.T. Baxter[1], M.S. Stewart[2], K. Breker[1], M.L Fassbender[1], A. Krätschell[3], S. Petersen[3]

[1]Department of Earth and Environmental Sciences, University of Ottawa, Ottawa, Ontario
[2]Department of Earth and Environmental Sciences, Mount Royal University, Calgary, Alberta
[3]GEOMAR-Helmholtz Centre for Ocean Research Kiel, Kiel, Germany

Introduction

Volcanism within back-arc settings is commonly thought to be restricted to narrow axial neovolcanic zones that bear similar characteristics to seafloor spreading at mid-ocean ridges. However, magmatic output within back-arc basins varies spatially and temporally due to the interplay between plate kinematics, large-scale mantle dynamics and subducting slab properties (e.g., Sdrolias and Müller, 2006). Recent studies using high-resolution bathymetry show that there is a high degree of variability in both the style and volume of magmatic activity within modern back-arc basins (e.g., Anderson et al., 2017). To better understand crustal accretion in modern back-arc basins, we used remote predictive mapping (RPM) techniques to construct a geological map of the Rochambeau Rifts (RR) region in the northwestern Lau Basin, at 1:200,000. The RR are a complex series of back-arc spreading centers and volcanoes responsible for voluminous magmatism in the region. We examine the volcanism, structure and crustal makeup of the RR and relate the magmatic output to both the localized stress regimes as well as the far-field stresses within the larger microplate framework of the Lau Basin.

Tectonic Setting

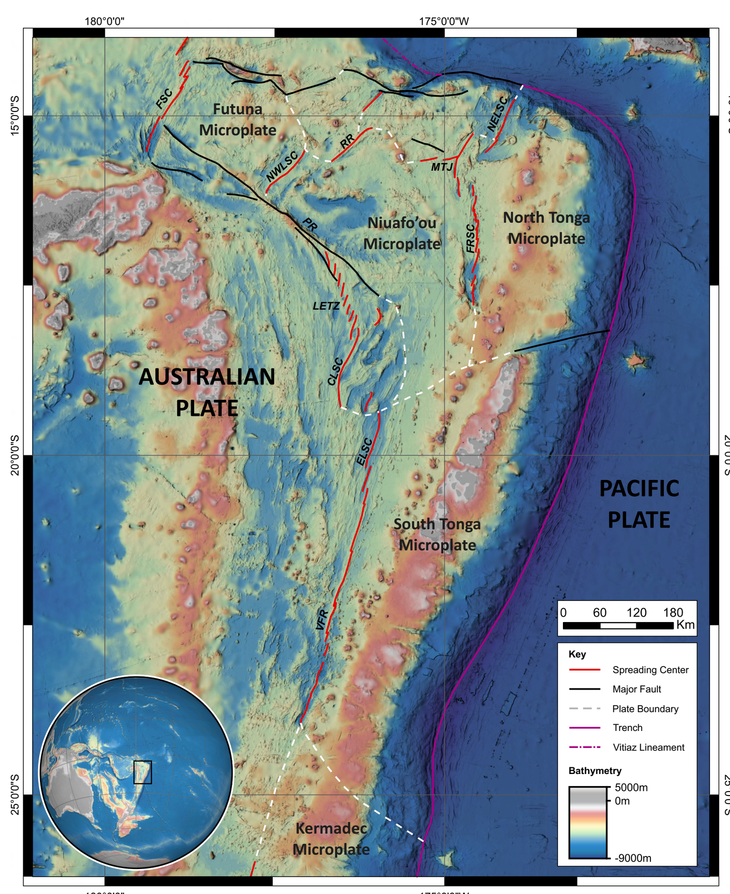

Figure 1 Adapted from Baxter et al. (2020). Regional bathymetric map of the Lau Basin displaying active spreading centers, and major microplate boundaries (Bird, 2003). FSC = Futuna Spreading Centre, NWLSC = Northwest Lau Spreading Center, RR = Rochambeau Rifts, MTJ = Mangatolu Triple Junction-southern arm, NELSC = Northeast Lau Spreading Center, LETZ = Lau Extensional Transform Zone, FRSC = Fonualei Rift and Spreading Center, CLSC = Central Lau Spreading Center, ELSC = Eastern Lau Spreading Center.

The Lau Basin (Fig 1) is an active back-arc basin which formed after rifting of the Lau-Tonga paleoarc ~6 Ma (Hawkins, 1995). Its distinctive V-shape formed due to a southward propagating rift, with increasing tectonic complexity from south to north, reflecting the oblique convergence of the Pacific Plate, the collision with the Melanesian Borderland Plateau and interaction with the Samoan plume.

The structural evolution of the Lau Basin was originally portrayed as a three-plate kinematic model, dominated by the Niuafo'ou, Tonga, and Futuna microplates (Zellmer and Taylor, 2001), with variations on this model published by Conder and Wiens (2011), and Sleeper and Martinez (2016). Numerous other microplates (and so-called nanoplates) have since been defined along the northern margin of the basin between the Futuna Fracture Zone and the Peggy Ridge Transform (e.g., Stewart et al., 2022). The various microplates have borders that are defined by numerous active spreading centers and/or transform zones. The spreading segments vary in length, shape and spreading rates, which we have correlated with magmatic output.

Methodology

Remote predictive mapping (RPM) was used to create the 1:200,000 geological map of the RR. This involves the compilation of several remotely acquired geoscience datasets that overlap the mapping area and together can be used to interpret volcanic geomorphology and structure. Ship-based multibeam echosounder (MBES) bathymetry and backscatter data (Fig 2), as well as other regional scale geophysical datasets, were among those used to identify map units and seafloor volcanic features. MBES data were collected during the R/V Southern Surveyor SS2008-07 and SS2009-02 cruises, with grid resolutions of 30 m and 35 m respectively (Arculus, 2008; Arculus, 2009). MBES data cover approximately 87% of the mapping area; ship-based multibeam was combined with Global Multi-Resolution Topography (GMRT; Ryan et al., 2009) for regions with incomplete multibeam coverage. The overall workflow and legend for back-arc basin formations follow Stewart et al. (2022). The map boundaries correspond to the Rochambeau Assemblage, defined by several geological formations that are grouped in terms of their origin, lithology, inferred age, and tectonic and structural regime (Stewart et al. (2022). Volumes were calculated using an ArcGIS polygon volume function, where volumes are determined above a minimum elevation value (Zmin).

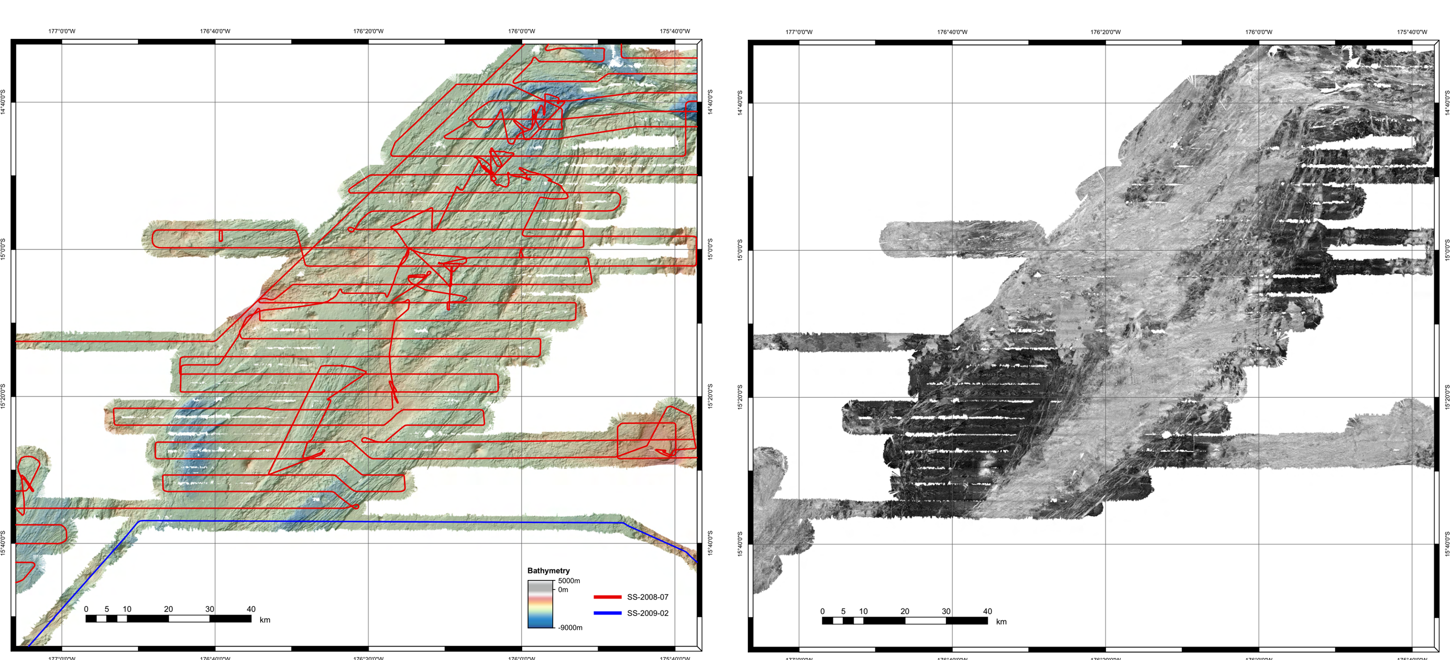

Figure 2 Available shipboard MBES data used for mapping Rochambeau. A) Shipboard bathymetry compilation from the RV *Southern Surveyor* cruises SS2008-07 and SS2009-02 cruises. Shiptrack lines are overlain in red and blue. B) Acoustic backscatter data collected during the RV *Southern Surveyor* SS2008-07. Signal strength is related to seafloor reflectivity.

Rochambeau Geologic Map

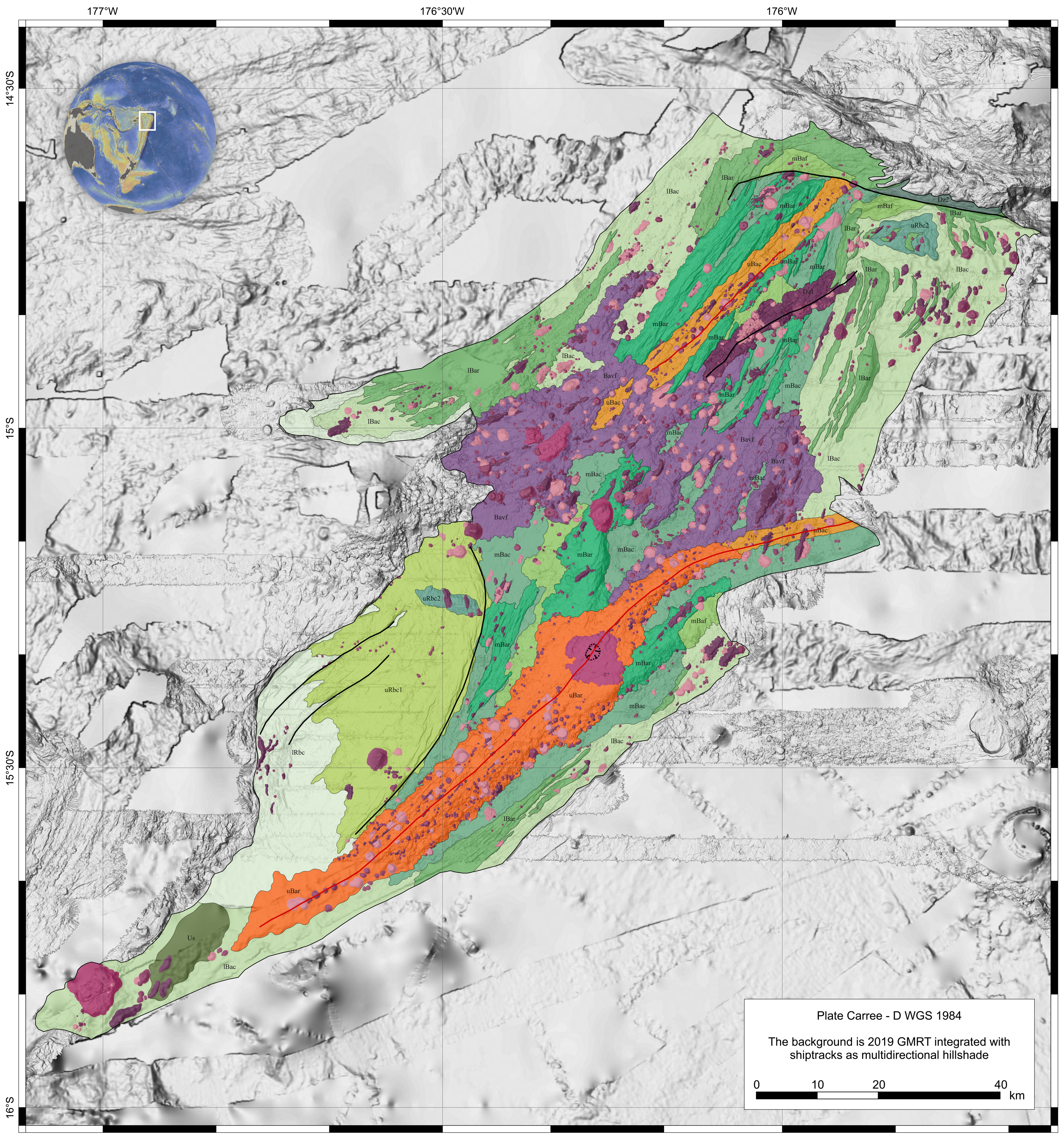

LABEL	UNIT NAME AND DESCRIPTION
	BACKARC VOLCANOES
Bav1	**Conical volcano** Cone-shaped edifice composed of lava flows and volcaniclastic material extruded onto older crust, commonly with a summit crater or caldera and/or cut by dike complexes (width:height ≤5)
Bav2	**Shield volcano** Mound-shaped edifice composed of lava flows extruded onto older crust, commonly with a central caldera (width:height >5)
Bav3	**Dome volcano** Dome-shaped edifice composed of lava flows extruded onto older crust, may have a flat-topped surface, summit crater, central dike or be tectonized (length:width ~1)
Bav4	**Fissure volcano** Elongated volcanic edifice composed mostly of lava flows extruded onto crust, commonly with a central dike (length:width >3)
Bavf	**Volcanic field** A broad area of lava flows and volcaniclastic material surrounding a number of closely-spaced volcanoes
	BACKARC RIFTS AND SPREADING CENTERS
Upper	
uBar	**Axial backarc volcanic ridge** Volcanic ridge marking the active spreading center consisting of lava flows, small volcanic edifices (cones and domes), dike complexes and calderas
uBac	**Axial backarc crust** Undivided backarc crust in the inner rift valley of an active spreading center
Middle	
mBar	**Proximal volcanic or tectonic ridge** Elongated volcanic edifice or coalesced ridges in the outer rift valley or on the flank, adjacent to an active spreading center or axial volcanic ridge
mBac	**Proximal backarc crust** Undivided backarc crust in the outer rift valley, adjacent to an active spreading center or axial volcanic ridge (may include products of off-axis volcanism)
mBaf	**Backarc rift flank** Undivided backarc crust on the flank of the outer rift valley, including volcanic ridges, volcaniclastic material, and flows (may include products of off-axis volcanism)

LABEL	UNIT NAME AND DESCRIPTION
	BACKARC RIFTS AND SPREADING CENTERS - Continued
Upper	
lBar	**Distal volcanic ridge** Elongated volcanic edifice or coalesced ridges on distal backarc crust (may include products of off-axis volcanism or earlier seafloor spreading from a distant ridge; commonly obscured by volcaniclastic cover)
lBac	**Distal backarc crust** Undivided backarc crust beyond the outer rift valley and flank of an active spreading center (may include products of off-axis volcanism)
	RELICT BACKARC
Upper	
uRbc1	**Upper relict backarc crust** Undivided backarc crust outside an identifiable area of active spreading (may be a product of intraplate volcanism, rifting of earlier backarc crust, or an unknown spreading center)
uRbc2	**Tectonized relict backarc crust** Intensely deformed backarc crust outside and identifiable area of active spreading
Middle	
lRbc	**Lower relict backarc crust** Earliest exposed extrusive and intrusive rocks in the backarc and outside and identifiable area of active spreading
	OTHER BACKARC FORMATIONS
Us	**Seamount** Volcanic or tectonic edifice of undetermined origin
Dz1	**Volcanic deformation zone** Fault controlled zone of lineated volcanoes, lava flows and deformed crust
Dz2	**Deformation zone** High-strain zone commonly associated with transcurrent faults (likely of crustal scale)
	SYMBOLS
	Caldera ring fault; Spreading center; Major fault

Figure 3 Geological Map of the Rochambeau Rifts, showing the identified formations. The youngest backarc crust is located along the two spreading axes (orange) and is surrounded by older backarc crust (green) and volcanoes/volcanic flows (pink and purple). The legend used for this map was adapted from the geological legend of the Lau Basin by Stewart et al. (2022).

Crustal Architecture and Magmatic Productivity

The mapped area of the Rochambeau Rifts (~8155 km^2) is dominated by active backarc crust separated into two zones of active spreading in the north and south. Approximately 15% (~1186 km^2) of the active back-arc crust is covered by volcanic flow fields (Bavf) that total ~367 km^3 of volcanic material. These flow fields separate the northern and southern segments of active spreading. The northern segment is defined by a 60-km long rift zone floored by 76.4 km^3 of upper backarc crust (uBac) which defines the neovolcanic zone. The southern segment is defined by 120-km long axial volcanic ridge (uBar) with a total volume of 704.4 km^3. More than 2500 individual volcanoes have also been mapped within the RR Assemblage area, including 1801 volcanic cones, 400 fissure volcanoes, 325 dome volcanoes, and 6 large shield volcanoes. The volcanoes represent a total volume of 167.5 km^3, or nearly 15% of the total magmatic budget of the RR Assemblage, and are dominated by shield volcanoes (59.1 km^3), followed by domes (44.7 km^3), cones (32.4 km^3), and fissures (31.3 km^3). Considering the volume of material from the neovolcanic zones, all the discrete volcanoes and that of the central flow fields, the melt flux for the RR is estimated to be 0.06 km^3/yr. This calculation is based on spreading rate age estimates using the widths of the neovolcanic zones for the northern and southern segments and assumes that all the discrete volcanoes have erupted within the last 10,000 years.

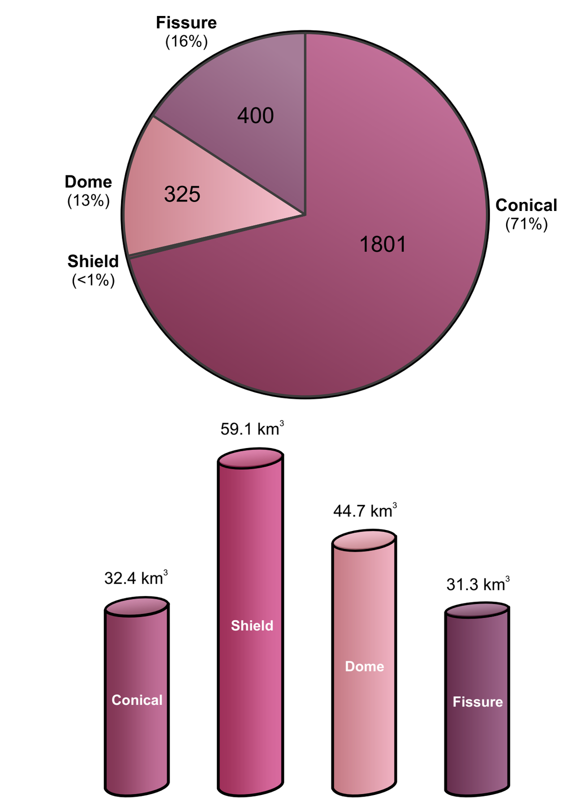

Figure 4 Quantitative summary of all mapped volcanoes in the Rochambeau Rifts. A) Numerical abundances and percentages by volcano type. B) Volumetric totals by volcano type. Cylinders are proportionally scaled to relative volume quantities

Structural Controls

Differing styles of volcanism between the northern and southern halves of the RR assemblage is partially attributed to varying fault densities (Fig 5) between the two areas. Faulting is concentrated in the northern rift segments, highlighting greater crustal permeability in the north of the assemblage. The highest fault densities are located immediately adjacent to the northern rift segment, with far fewer faults in the south. This is consistent with the more abundant off-axis volcanism in the north compared to the south where most of the volcanism is channeled along the neovolcanic zone to form the axial volcanic ridge. The high fault densities in the north result in the more diffuse off-axis volcanism that is observed here.

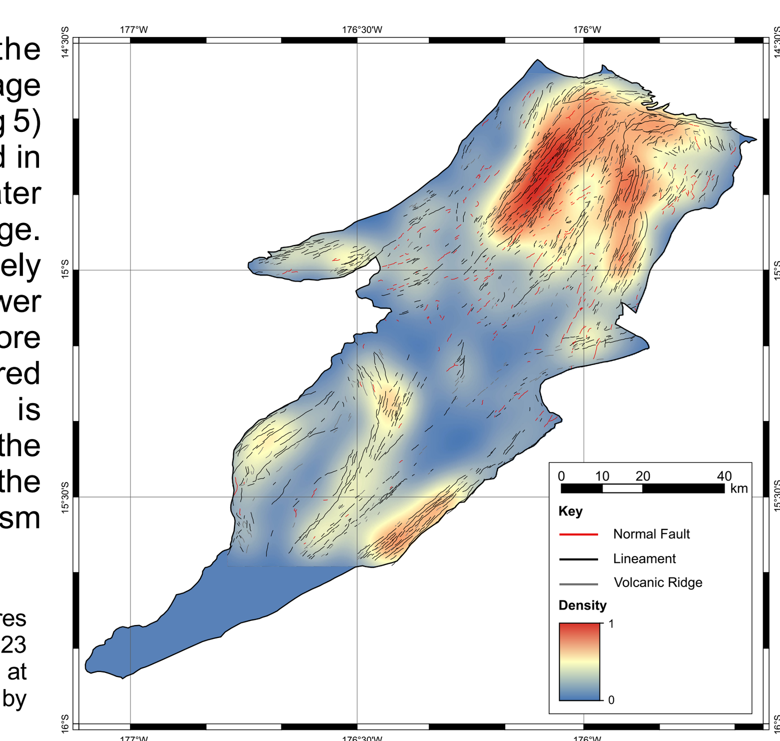

Figure 5 Density contours of structures in terms of identified structures per km^2, based on a 10-km search radius. Overlayed are 1623 digitized structures (minimum strike length of 200m) mapped at 1:50,000 and assembled in ArcGIS. Structures are categorized by type in accordance with their geometric properties.

Conclusions

The total magmatic output of the RR is estimated to be ~0.06 km^3/yr. Global melt production at mid-ocean ridges averages 18-21 km^3/yr (Deligne and Sigurdsson, 2015), or approximately 0.03 km^3/yr for every 100 km of ridge length. Thus, magmatic productivity at the RR is nearly double that of a similar-sized MOR segment. Additionally, different magma focusing mechanisms in the northern and southern halves of the RR account for different eruption rates, with diffuse off-axis volcanism observed in the north accounting for 0.25 km^3/yr vs. the axial backarc volcanic ridge in the south accounting for 0.35 km^3/yr. The different controls on volcanic eruptions observed in the RR may also have played a role in the voluminous magmatic productivity in some ancient greenstone belts. Understanding these processes has important implications for mineral exploration owing to the close relationship between magmatic productivity, crustal permeability, and mineral endowment. We further suggest that certain areas within the Rochambeau Rifts may contain many of the crucial components necessary for, as of yet undiscovered, Seafloor Massive Sulfide (SMS) deposits.

Acknowledgements

This research is a product of the Metal Earth Project funded by the Canada First Research Excellence Fund (CFREF), the iMAGE-CREATE Project funded by Natural Sciences and Engineering Research Council of Canada (NSERC), and the Marine Mineral Resources Group at the GEOMAR Helmholtz Centre for Ocean Research Kiel. The Helmholtz Association, NSERC, and CFREF are acknowledged for the support of this work through research grants and project funding to the authors. This is contribution MERC-ME-2022-04 to the modern-ancient crust project of the Canadian Metal Earth program.

Anderson, M. O., Chadwick, W. W., Hannington, M. D., Merle, S. G., Resing, J. A., Baker, E. T., … Augustin, N. (2017). Geological interpretation of volcanism and segmentation of the Mariana back-arc spreading center between 12.7°N and 18.3°N. *Geochemistry, Geophysics, Geosystems*, *18*(6), 2240–2274.
Arculus, R. J. (2008). Voyage Summary SS07/2008 Northern Lau Vents Expedition.
Arculus, R. J. (2009). Voyage Summary SS02/2009 Hydrothermal plume and structural geology mapping in the Tonga/Fiji region.
Baxter, A. T., Hannington, M. D., Stewart, M. S., Emberley, J. M., Breker, K., Krätschell, A., Petersen, S., Brandl, P. A., Klischies, M., Mensing, R., Anderson, M. O. (2020). Shallow seismicity and the classification of structures in the Lau back-arc basin. *Geochemistry, Geophysics, Geosystems*, *21*, e2020GC008924.
Bird, P. (2003). An updated model of plate boundaries. *Geochemistry, Geophysics, Geosystems*, *4*(3).
Deligne, N. I., & Sigurdsson, H. (2015). Global rates of volcanism and volcanic episodes. In Sigurdsson, H., Houghton, B., Rymer, H., Stix, J., McNutt, S. (Eds.) *The Encyclopedia of Volcanoes* (2nd ed., pp. 265-272). Elsevier.
Hawkins, J. W. (1995). The geology of the Lau Basin. In *Backarc Basins* (pp. 63-138). Springer.
Ryan, W. B. F., S.M. Carbotte, J. Coplan, S. O'Hara, A. Melkonian, R. Arko, R.A. Weissel, V. Ferrini, A. Goodwillie, F. Nitsche, J. Bonczkowski, and R. Zemsky (2009), Global Multi-Resolution Topography (GMRT) synthesis data set, *Geochem. Geophys. Geosyst.*, 10, Q03014.
Sdrolias, M., & Müller, R. D. (2006). Controls on back-arc basin formation. *Geochemistry, Geophysics, Geosystems*, *7*(4).
Stewart, M. S., Hannington, M. D., Emberley, J., Baxter, A. T., Krätschell, A., Petersen, S., Brandl, P. A., Anderson, M. O., Mercier-Langevin, P., Mensing, R., Breker, K., Fassbender, M. L. (2022). A new geological map of the Lau Basin reveals crustal growth processes in arc-backarc systems. *Geosphere*, *18*(2), 910-943.
Zellmer, K. E., & Taylor, B. (2001). A three-plate kinematic model for Lau Basin opening. *Geochemistry, Geophysics, Geosystems*, *2*(5).